We are IntechOpen, the world's leading publisher of Open Access books Built by scientists, for scientists

4,800
Open access books available

122,000
International authors and editors

135M
Downloads

Our authors are among the

154
Countries delivered to

TOP 1%
most cited scientists

12.2%
Contributors from top 500 universities

CLARIVATE ANALYTICS BOOK CITATION INDEX INDEXED

WEB OF SCIENCE™

Selection of our books indexed in the Book Citation Index in Web of Science™ Core Collection (BKCI)

Interested in publishing with us?
Contact book.department@intechopen.com

Numbers displayed above are based on latest data collected.
For more information visit www.intechopen.com

6

Introduction of Neutron Diffractometers for Mechanical Behavior Studies of Structural Materials

E-Wen Huang[1], Wanchuck Woo[2] and Ji-Jung Kai[3]
[1]*Department of Chemical & Materials Engineering and Center for Neutron Beam Applications, National Central University*
[2]*Neutron Science Division, Korea Atomic Energy Research Institute*
[3]*Department of Engineering and System Science, National Tsing Hua University*
[1,3]*Taiwan*
[2]*South Korea*

1. Introduction

The design of advanced metallic materials for their structural applications requires the understanding of the strengthening mechanisms and property evolution subjected to different types of deformation modes[1]. These metallic systems can interact with their microstructure upon the changes of the environmental conditions, such as strain rate and temperature[2]. While the microstructure has been facilitated for many purposes, this chapter puts forward how to characterize the structural properties with neutron diffractometers. Moreover, nowadays, many neutron diffractometers are equipped with load frames, which advance the diffraction measurements to real-time observations. The chapter considers that deformation mechanisms and their effects on the microstructure are central to the mechanical behavior of structural materials. The main objective of the chapter is to introduce readers how to facilitate the neutron diffractometers to study the mechanical behavior of the structural materials. The reported diffractometers are summarized from the literatures, public information, and on-site visits. Some useful software for diffraction-profile and scattering-intensity analyses is briefly mentioned. The microscopic features are connected with the macroscopic states, such as the applied stresses and temperature evolution to bridge the understanding of the bulk property. What reciprocal information obtained from the diffraction profiles can be inferred to the materials structural parameters will be explained.

2. Neutron diffraction and diffraction-profile-refinement software

Neutrons are elementary particles with a finite mass (m, about 1.67×10^{-27} kg) and spin, without an electron charge. It carries a magnetic moment, and according to *de Broglie* law, the neutrons behave like waves with a wavelength (λ) at the levels of Å and gives rise to diffraction[3]. Neutron diffraction is based on the nuclear interaction between neutrons and the matters and on magnetic interaction with magnetic moments of the atoms due to its magnetic moments. Specifically, in this chapter, we focus only on the application of the

elastic neutron scattering. Moreover, for the applications of the neutron diffractormeters to characterize the polycrystalline metallic systems are based on the idea of the powder diffraction. The concept of a powder diffraction experiment is that the sample consists of a large number of small randomly oriented crystallites. If the number is sufficiently large, there are enough crystallites in various diffracting orientations to yield diffraction patterns. Depending on the microstructure arrangements, interferences between the scattered neutrons are constructive when the path difference between diffracted rays differs by an integral number of wavelengths. This is described by the well-known Bragg equation. There are various methods to refine the aforementioned scattering distribution function. The General Structure Analysis System (GSAS)[5] based on full-pattern Rietveld analysis method[6] is one of the most popular peak-profile-refinement software. The users of GSAS[5] can obtain peak-position, intensity, peak profiles and width, respectively with the model fitting. In the following sections, the refinement of the peak position, intensity, width and their related materials microstructure are introduced in Sessions 2.1, 2.2, and 2.3, respectively.

2.1 Peak position, lattice strain, and using lattice strain for mechanical behavior study

With the single-peak refinement of the GSAS, peak positions (d^{hkl}) of specific lattice plane can be refined for the calculations of the lattice strain, ε^{hkl}, as shown in Equation (1):

$$\varepsilon^{hkl} = \frac{d^{hkl} - d^{hkl}{}_0}{d^{hkl}{}_0} \times 10^6 (\mu e) \,. \tag{1}$$

The refined peak positions of each *hkl* are calculated according to the changes in the *d*-spacing (d^{hkl}). The lattice evolution is relative to the initial *d*-spacing ($d^{hkl}{}_0$) as a function of the deformation levels.

The lattice-strain evolution results can be referred to the generalized Hooke's law to compare the measured results with the classic models. For examples, the relationship between the stress and strain is one of the most fundamental properties of the materials. The Hooke's law presents the strength of interatomic forces between adjacent atoms. The reversible nature of the bulk materials is known as the elastic strain. Hooke's law can be generalized relative to the loading directions. As a stress is applied in one direction (for example, the Y-direction) of the materials, it could yield strains in the X, Y, and Z-directions. Hence, the Poisson's ratio (υ), and the modulus of elasticity (E), and the stiffness can also be determined by knowing the peak position changes upon elastic deformation.

Furthermore, with careful experimental setup, the elastic constants vary as a function of the crystallographic orientation, the strains in each direction subjected to three normal and six shear stress components, can be measured, too. For examples, the cubic crystals, described in Equation 2, have three independent elastic constants and different direction cosines relative to the crystallographic directions.

$$\frac{1}{E} = s_{11} - 2\left[\left(s_{11} - s_{12} \right) - \frac{1}{2} s_{44} \right] \left(l_1^2 l_2^2 + l_2^2 l_3^2 + l_1^2 l_3^2 \right) . \tag{2}$$

l_1,l_2 and l_3 are direction cosines. The direction cosines for principal directions in a cubic lattice can be referred to Hertzbug's book, where the theoretical models are clearly

described[7]. This is one of the examples of how to apply neutron diffractometers to calculate the fundamental materials properties. Besides, the fundamental stress-strain relationships, several recent studies show that the lattice strain can be inferred to the thermomechanical behavior[8,9]. Following is a short review of this latest application of neutron peak position data.

2.1.1 Lattice strain for thermomechanical calculations

The state of solids can be described by the strain (ε) or stress (σ) and temperature (T). Under the Hooke's law, the stress- or strain-temperature relation can be derived from the laws of thermodynamics (Stanley and Chan 1985 [10]) as

$$\Delta T = \left(-K \frac{ET}{1-2\upsilon} \Delta\varepsilon \right) \text{ or} \tag{3}$$

$$\Delta T = \left(-KT\Delta\sigma \right). \tag{4}$$

T is the absolute temperature of the current state, and K is a material constant [$K = \bar{\alpha} / \rho C_V$]. Other parameters, $\bar{\alpha}$ is the coefficient of the linear thermal expansion, ρ is the mass density, and C_v is the specific heat at a constant volume. $\Delta\varepsilon$ is the change of the strain, and $\Delta\sigma$ is the change of the stress. υ is the Poisson's ratio. In Equations 3 and 4, the temperature response is negatively proportional to the change in the stress or strain states of a homogenous elastic solid.

It has long been recognized that the mechanical energy can be separated into the stored energy of cold work and thermal energy[11]. Einstein's, Debye's, and Grüneisen's models[12] unify the elastic deformation with thermodynamics. New approaches are proposed to model the stored energy of the deformed microstructure[13-15].

To answer the temperature-lattice strain relationships posed above, Huang et al[9]. applied the lattice strain evolution subjected to cyclic loadings with Wong et al.[13] and Quinn et al.[16]'s thermo-mechanical relationship as described in Equation 5:

$$\Delta T = \frac{-\alpha T}{\rho C} \left(1 - \frac{1}{\alpha E^2} \frac{\partial E}{\partial T} \sigma_m \right) \Delta\sigma \ . \tag{5}$$

ΔT is the temperature response subjected to the mechanical deformation. α is the thermal expansion. C is the heat capacity. E is the Young's modulus. σ_m is the residual stress introduced by the plastic deformation. $\Delta\sigma$ is the stress change due to the elastic deformation, which can be referred in Huang *et al.*'s study[9] as the lattice-strain evolution. Based on their measured lattice strain, the thermo-mechanical responses were estimated with the modified Stanley and Chen's equation[10]:

$$\Delta T = \frac{-\alpha E_{111} T}{\rho C (1-2\upsilon)} \left(\frac{\varepsilon_{111}^{loading} + \varepsilon_{111}^{transverse}}{2} \right) \times \frac{Volume\ of\ the\ Deformed\ Specimen}{Whole\text{-}specimen\ Volume} \tag{6}$$

E_{111} is the 111-lattice plane modulus[17]. ν is the Poisson ratio. Because after cyclic loading, there is practical no texture development in the studied system, the lattice strains (ε_{111}) of

grains in orthogonal directions (oriented to loading and transverse directions, respectively) can be averaged. Thermal expansion ($\alpha = \frac{\gamma \rho C_V}{3E}$) is a function of Grüneisen parameter ($\gamma \equiv \frac{\partial\left(ln\,\omega_{Debys}\right)}{\partial\left(ln\,V\right)}$), where ω_{Debys} is Debye frequency and V is the volume. Based on the generalized Hooke's law, the temperature responses can be calculated with the updated volume strain[11] as $\Delta V = (1+\varepsilon_{111})(1-\upsilon\varepsilon_{111})^2 - 1$. Huang *et al.*[9] show that the calculated and the measured temperature-evolution trends qualitative agree with each other. Certainly, there is quantitative discrepancy because during the deformation, the plastic deformation occurred, but not counted in the above elastic-based calculations. Moreover, in Huang *et al.*'s 2010 work[8], their thermal resistivity calculations also validate the above approach of the use of lattice strain to understand the thermomechanical behviors. Besides the above lattice strain applications, to explore the plastic deformation, the following two sections will introduce how to correlate the peak intensity for materials texture and the peak width for microstructure studies, respectively.

2.2 Diffraction-peak intensity and texture

The diffraction is a Fourier transformation from the crystal space into the reciprocal space. Intensities of various *I(hkl)* of the crystalline systems are proportional to the squares of the crystallographic structure factors *F(hkl)*.

h k l are the Miller indices of the unit cell.

The peak intensity can be fitted from the individual *hkl* peaks. The normalized intensity evolution as a function of stress can be calculated using Equation (7) to trace the texture development through the bulk deformation.

$$I_{hkl} = \frac{I^{deformed}{}_{hkl}}{I^{0}_{hkl}} \tag{7}$$

2.2.1 Combining intensity evolution for texture development and lattice-strain changes for self-consistent modeling

In polycrystalline materials, the orientations of the grains decide the texture of the materials. Under plastic deformation, slips on specific crystallographic planes produce lattice rotations which accumulate texture. Hill's [18] and Hutchinson's[19] self-consistent (SC) models have been applied very successfully to simulate the texture development of polycrystalline materials[20] by the lattice-strain evolution based on neutron-diffraction measurements via the Elasto-plastic self-consistent (EPSC) model for several metallic materials[21, 22]. The intrinsic assumptions of the EPSC model consider the active inelastic-deformation mechanisms, and, hence, the stiffness/compliance constants are important for simulations[23-25]. The present session review Huang *et al.*'s work[17], which extends SC modeling to moderate-to-large deformation strain, considering the grain rotation for describing preferred grain-orientation distributions. Huang *et al.* applied Wang's[26-28] visco-plastic self-consistent (VPSC) model to simulate the texture development, based on their measured lattice strains and macro stress-strain responses from a nickel-based alloy. The VPSC model considers the activity of slip

systems and its influence on grain rotation[25]. The VPSC code is based on Wang's fundamental work[26-28]. With the neutron diffractometers, the *in-situ* experimental macro/lattice stress-strain curves can be used as an input to simulate the texture and the probability of the active-slip systems from the multiple *hkl*-reflections. A VPSC model was implemented for estimating the distribution of microstresses and texture evolution in Huang *et al*.'s work[17]. All the parameters were derived by fitting the diffraction profiles of the experimental neutron measurements. The compliances used in the simulations can be calculated from the measurement of lattice-strain (ε_{hkl}) within the elastic deformation. There is good qualitative agreement in the inverse pole figures from the measured intensity evolution to the simulated results. Meanwhile, the quantitative discrepancy suggests that during the plastic deformation of the structural materials, besides the considerations of the lattice evolution and texture development, we need also to take into account the effects of microstructure changes.

2.3 Peak-profile analyses and microstructure changes

Practically, structural polycrystalline materials contain imperfections that influence the intensity of the Bragg reflections distributions. The main deviations observed in the diffraction profiles are from microstructure and from the strain and stress in the sample. The Rietveld method[29] is a breakthrough method to resolve the peak profiles by facilitating the full pattern profiles with the crystal structure refinements. The Rietveld method is a least-square fit of a given profile function to the diffraction pattern by minimizing the difference between the observed and calculated diffraction intensity distributions:

GSAS has three classical profile-shape functions for the users to refine the diffraction profiles. They are the Gaussian, the Lorentzian, and the Pseudo-Voigt-type distribution functions. Typically, the crystalline-size broadening produces Lorentzian distribution-type tails in the peak profile, while microstrains produce Gaussian distribution-type contributions. Full-width-at-half-maximum (FWHM) values are significantly affected with such characteristics.

As a general rule, the determination of a particle size is treated by the Scherrer equation[4]. The Scherrer equation gives a rough estimate of the broadening caused by the crystalline size. The strain broadening can be covered by the Gaussian, which has a width proportional to $\tan(\Theta)$ [30]. Using GSAS, the peak-width can be decomposed into the Gaussian and Lorentzian broadening components simultaneously.

2.3.1 Microstructure for mechanical behavior study

From a mechanistic perspective, the creation of obstacles to the dislocation motion can enhance the strengthening mechanisms. These obstacles provide additional resisting force above the intrinsic lattice friction. The strengthening mechanisms are revealed macroscopically through a larger flow stress[11]. Hence, it is important to examine how the microstructures create the obstacles to the motion of the dislocations.

The cold work on the material can be presented by the microstructural changes at the dislocation level. The increase in the dislocation density can alter the mechanical properties. From the basic observation of generic crystalline solids, the polycrystalline materials are composed of many different grains, each with a particular crystalline orientation and

separated by grain boundaries[31]. The grains and the associated boundaries make up the polycrystalline microstructure, such as the grain size and patterned-dislocation structures[32]. In a worked material, the microstructure is characterized by a series of heavily dislocated grains[33].

The microstructures with the defects can significantly change the strengths of the materials[34]. Hence, it is one of the most important structural materials properties for their mechanical applications. Among different perspectives, the material's microstructure must account for the dislocations. In a broad term, the dislocations play the main role of the permanent deformation of crystalline solids largely because the dislocations are the primary means of the plastic deformation[11]. The attempt to monitor such plasticity can be based upon different methods. At the smallest scales, the morphology can be observed by the atomic structure of dislocations via transmission-electron microscopy (TEM) [35].

2.3.2 Microstructure and peak-profile changes in the plastically-deformed materials

To bridge the texture and microstructure developments subjected to plastic deformation, in this session, we continue review Huang *et al*.'s work[17]. Huang *et al*. assume that during the formation of a hierarchical dislocation structure in the plastically-deformed material, some part of a dislocations group within dislocation walls and some part remain randomly distributed. The formation of the hierarchical dislocation structure in many metallic polycrystalline materials under different deformation has been widely reported[35-39]. Readers may refer to Zehetbauer[40], Schafler *et al*.[41], and Hughes and Hansen[42]'s description of the formation of the hierarchical dislocation structure to visualize that with the dislocation walls creating, there are certain misorientations/tilt/twist between the neighboring regions of the same grain and some other random portion of the dislocation population randomly distributed between the walls. There is practically no misorientation/tilt/twist in the interior. For simplicity, the dislocation walls can be assumed to be composed from the equidistant-edge-dislocations. Meanwhile, the screw dislocations remain randomly distributed in the cell interior. Hence, as presented previously[43-46] equidistant-dislocations walls can result in the Lorentzian type of broadening. The randomly-distributed or weakly correlated dislocations in the interior can result in the Gaussian type of broadening. Above all, the readers can base on the microstructure results of their observations and then apply a proper peak-profile function of the GSAS to correlate the refined neutron diffraction results to the microstructure evolution.

2.4 Small-angle neutron scattering and the precipitation strengthening

Finally, in the end of the introduction of the relationship between structural materials microstructure and neutron instruments, the author would like to review how to investigate the precipitates of the metallic alloys. The age-hardening effect of the precipitates has been extensively used to improve the mechanical behavior by impeding the dislocation movements in various metal-based structural materials[47].

If there is a supersaturation of substitutional impurities, subsequent annealing will lead to the formation of precipitates[38]. The precipitates can act as the obstacles to the dislocations. Specifically, the equilibrium of two-phase coexists between the matrix phase and a second phase. The presence of such second-phase particles makes itself known through a substantive change in the mechanical properties of the material. Observations on

precipitation hardening make it evident that the key microstructural features in this context are the mean particle radius and the volume fraction of such precipitates[11]. In particular, the variation in the flow stress is a function of particle size. The particle-cutting mechanism is dominant at small radii. The Orowan process is easier at large particle radii[34].

The age-hardening effect was discovered by Wilm[48]. Since then, it has been extensively used for developing various metal-based structural materials for industrial applications. The strengthening mechanism relies on the precipitation in some phases other than that of uniform dispersion. The dislocations are localized and prevented from continued movements by the strain field introduced by the lattice mismatch between the precipitates and the homogeneous matrix. The morphology of the precipitates and their spatial arrangement in the embedded matrix are two known key elements in deciding the mechanical performance.

The small-angle neutron scattering (SANS) approach presents a complementary tool to the microscopy technique. It provides the nano-scale information via the measurement of the Fourier transform of the spatial correlation function. The collected scattering intensity, *I(Q)*, is presented in reciprocal *Q* space. Therefore, to obtain quantitative real-space information, model fitting is usually required. In this chapter, we review Chen *et al.*'s model[49] for SANS *I(Q)* study of precipitation strengthening. In general, *I(Q)* obtained from a system consisted of nonspherical particles can be expressed as

$$I(Q) = \frac{N|\Delta\rho|^2}{V_S} P(Q)\left\{1 + \beta(Q)\left[S(Q) - 1\right]\right\} + I_{\mathrm{INC}} \tag{8}$$

where Δρ is the difference in scattering-length densities between the particle and the dispersion medium; V_S, the sample volume illuminated by neutron beam; *N*, the number of precipitates in V_s; *P(Q)*, the average form factor given by the shape and density profile of particles; *S(Q)*, the effective one-component inter-precipitate structure factor, which is a measure of the inter-particle interference; *β(Q)* the decoupling constant dependent on both the size polydispersity and intra-precipitate density profile[50], and $I_{\mathrm{INC}}$the incoherent background.

In the practical implementation of the introduced model fitting, $\frac{N|\Delta\rho|^2}{V_S}$ is treated as a fitting parameter suggested by Pedersen[51]. The shape of the polydisperse precipitate can be modeled by the form factor, *P(Q)*. The effect of polydispersity can be incorporated through the decoupling approximation and a standard Gaussian law[50].

$$N(x, R, \delta) = \frac{1}{\sqrt{2\pi\delta^2}} \exp\left[\frac{-(x-R)^2}{2\delta^2}\right] \tag{9}$$

where *R* is chosen to describe the size distribution (δ is the variance).

In Huang *et al.*'s exemplary system[49], the inter-precipitate structure factor, *S(Q)*, is calculated via a stochastic phenomenological model. It is assumed that precipitates are partially ordered and separated from the nearest neighbors with a preferred distance, *L*, with a deviation measured by the root-mean square denoted by σ. The inter-precipitate structure factor[52], *S(Q)*, is expressed as a function of *Q*, *L*, and σ

$$S(Q,L,\sigma) = 2 \cdot \left\{ \frac{1 - \exp\left[-\left(Q^2\sigma^2\right)/4\right]\cos(QL)}{1 - 2\exp\left[-\left(Q^2\sigma^2\right)/4\right]\cos(QL) + \exp\left[-\left(Q^2\sigma^2\right)/2\right]} \right\} - 1 \quad (10)$$

Hence, the coherent SANS intensity distributions obtained from the alloys can be fitted by the above model and uniquely refine five parameters: R, ε, δ, L, and σ of the strengthening precipitates.

3. The neutron diffractometers for structural materials research

There are several neutron diffractometers in the world dedicated, but not limited, to the mechanical behavior study. Because this chapter focuses on the mechanical behavior study of structural materials, those diffractometers equipped with the load frames for *in-situ* measurements are summarized. In the following sessions, these neutron diffractometers are categorized into two groups and introduced according to their alphabetic order. The diffractometers located in the spallation neutron source facilities will be introduced in the session 3.1. The others located in the reactor neutron source facilities will be summarized in the session 3.2. The differences between the Spallation Neutron Source and Reactor Source are not the focus of this chapter. Here, only a brief comparison is summarized below.

For the time of flight, Spallation Neutron Source, a pulse of chopped neutrons illuminate the sample at different time. Within this range of the different time, the diffracted neutrons can cover several reflections of the materials within one pulse. With this unique feature, several *hkl* peaks can be revealed at almost "one time" simultaneously. This multiple-*hkl*-peaks-collection capability enables the researchers to easily characterize several phases with a wide range of the q-space at specific environmental at one pulse of the incident neutrons. On the other hand, the Reactor Source Neutron diffractometers can also cover similar range of the q-space, but with the adjusting of the monochromators and analyzers. Hence, it sometimes will take longer time for the Reactor Source to collect the same *hkl* diffractions than that of the Spallation Neutron Source. However, for the structure materials research with known representative *hkl* diffractions, most of the Reactor Source can provide very efficient lattice strain scans with better resolution to map the strain distribution for mechanical behavior study.

3.1 The engineering neutron diffractometers of the spallation neutron sources

3.1.1 ENGIN-X

Engin-X at ISIS, United Kingdom, is one of the most important engineering materials instruments of its kind. The ENGIN-X's two large detectors can collect the diffracted neutron intensity in two orthogonal directions simultaneously. The instrumental parameters can be referred to the ENGIN-X website of (http://www.isis.stfc.ac.uk/instruments/engin-x/engin-x2900.html). With *in-situ* capabilities for sample environments, ENGIN-X enables measurements on small volumes[53] to largesamples[54]. Historically, there are many important milestones research of the structure materials research carried out at the Engin-X[55].

3.1.2 SMARTS

Spectrometer for Materials Research at Temperature and Stress (SMARTS) is located in the beamline of the Los Alamos Neutron Science Center (LANSCE) [56] in the United States. The SMARTS is a third-generation neutron diffractometer constructed at the Lujan Center.

SMARTS provides capability on two important environmental conditions for mechanical behavior study. These two are the load frame and the furnace, which allow measuring the deformation under different types of loading modes and various temperatures. The furnace and load frame suite allows research on materials under extreme loads (250 KN) and at extreme temperatures (1,500°C) (http://lansce.lanl.gov/lujan/instruments/SMARTS /index.html). *In-situ* uniaxial loading on samples up to 1 cm in diameter at stresses of 2 GPa and with lower stresses at temperatures up to 1,500°C are routine. The importance of the two orthogonal detectors is evidenced in a magnesium-alloy research[57]. The appearance and the disappearance intensity evolution of the deformed magnesium-alloy shown in two orthogonal detectors demonstrate the kinetics of the twinning-detwinning. Furthermore, its space capability enables to perform *in situ* observation of temperature and stress evolution during friction-stir welding by Woo et al. [58]. Dr. Bjørn Clausen of the SMARTS create several very useful software for the usres' data deduction. One of them is the SMARTSware. The users can save a lot of time to refine the SMARTS data with SMARTSware.

3.1.3 TAKUMI

TAKUMI is a newly-built Engineering Materials Diffractometer located in Japan-Spallation Neutron Source. The real-space detecting range for the investigated materials covers from 0.5 to 2.7 Å (standard mode). TAKUMI also has a pair of orthogonal scattering-detector banks covering area in both of the horizontal and vertical directions. There large sample table has the load capacity up to 1 ton (http://j-parc.jp/MatLife/en/instrumentation/ ns_spec.html). TAKUMI has a loading machine to reach tension up to 50kN and 20kN with compression, respectively. The furnace of TAKUMI is designed to create the high-temperature environment up to 1273K.

3.1.4 VULCAN

VULCAN Engineering Materials Diffractometer at the Spallation Neutron Source of Oak Ridge National Laboratory (http://neutrons.ornl.gov/instruments/SNS/VULCAN/) has created the most various and extreme sample environment for its kind. Although it just opens to the general users since 2009, several new experiments, which were impossible before, have been carried out. New features are summarized below. VULCAN is the latest diffractometer in the world. Dr. Xun-Li Wang and Dr. Ke An build VULCAN's latest data acquisition software. With the most advanced software and flux, VULCAN creates real in-situ experimental environment, which can help the users to investigate the dynamics of the structural evolution subjected to mechanical deformation. VULCAN has the ability to study kinetic behaviors in sub-second times. VULCAN's rapid volumetric (3-dimensional) mapping can narrow a sampling volume down to 1 mm^3 with a measurement time of minutes. VULCAN also has very high spatial resolution (0.1 mm) in one direction with a measurement time of minutes. VULCAN can collect 20 well-defined reflections for in-situ loading studies simultaneously. Moreover, VULCAN is equipped with one of the most sophisticated load frame, which can even perform torsion experiments.

3.2 The engineering neutron strain scanning diffractometers of the reactor neutron sources

The strain scanners are mostly suitable for residual stress measurements but not limited to perform deformation behavior when the detector can be rotated for the appropriate

diffraction angle[59-62]. This type of the strain scanning instruments facilitates the concepts introduced in the session 2.1 to perform diffraction experiments. The diffraction peak positions determine the lattice parameters of the phases of the investigated engineering components. The importance of the strain mapping of the neutron diffractometers is that with the high-penetration of the neutrons, the gauged samples can be studied without the destructive specimen preparations. There are a number of research subjects performed with the aid of the strain scanning diffractometers for the understanding of the mechanical properties. Here we introduce a few examples, which have been published recently in literature: (1) Stress variation and crack growth around the fatigue crack tip under loading and overload[63, 64] (2) residual stresses, texture, and tensile behavior in friction stir welding[65, 66] (3) wavelength selection and through-thickness distribution of stresses in a thick weld[67] (4) residual stress determination in a dissimilar weld overlay pipe for the nuclear power plant applications[68] (5) Time-dependent variation of the residual stresses in a severe plastic deformed material[69]. In this session, we also summarize the various strain scanning diffractometers of the reactor neutron source for the mechanical behavior in the manner of alphabetic order.

3.2.1 KOWARI

KOWARI is a Strain Scanner of Australian Nuclear Science and Technology Organisation (ANSTO). KOWARI's advanced sample table can accommodate large objects (up to 1 tonne) and move them around reproducibly to within ~20 mm. With Australia's famous mining industry and the historical heritage of the Bragg Institute, KOWARI is building a program to serve for both of the commercial and academic users.

3.2.2 L3 Spectrometer

L3 Spectrometer of Canadian Neutron Beam Centre is mostly used for strain/stress mapping, crystallographic texture, grain-interaction stresses, precipitation and phase transformations (http://www.nrc-cnrc.gc.ca/eng/facilities/cnbc/spectrometers/l3.html). L3 can also be equipped with a stress rig for examining specimens under uniaxial load. For strain/stress mapping, a large variety of slit dimensions are available. L3 can also be equipped with a variety of sample orientation devices. The sample table with various translation and rotation devices can handle loads of up to 450 kg and provides a large 60 cm × 60 cm (2" × 2") platform. Stress Rig can provide uniaxial tension and compression load. Maximum applied load is 45 kN. L3 Spectrometer is famous for its industrial service and academic user communities for crystallographic texture and grain interaction measurements.

3.2.3 NRSF2

Neutron Residual Stress Mapping Facility (NRSF2) of the High Flux Isotope Reactor (HFIR) Oak Ridge National Laboratory is a strain scanning diffractometer open to the users. The wavelength can be chosen from a variety of monochromator crystal settings with a selection of wavelengths from 1.2 to 2.4 Å (http://www.sns.gov/instruments/HFIR/HB2B/). The high intensity HFIR enable the penetrating power of neutrons of the NRSF2 for scanning residual stresses in engineering materials.

3.2.4 RSI

Residual Stress Instrument (RSI) is a neutron-diffractometer at the High-flux Advanced Neutron Application Reactor (HANARO) of the Korea Atomic Energy Research Institute (KAERI). The diffractometer can measure three-orthogonal-direction strain components with high spatially-resolved sampling. Huang *et al.*'s recent work[70] shows the importance to measure all three directional strains for fatigue study of a stainless steel. RSI has two load frames up to 20 KN for the measurement of strains at room temperature and high temperature up to 800 °C. *In-situ* mapping is also available at the RSI of HANARO.

(1) FRM-II	http://www.frm2.tum.de/en/science/diffraction/stress-spec/index.html
(2) HANARO-RSI	http://nsrc.jaea.go.jp/aonetned/rsi.pdf
(3) HFIR-NRSF2	http://www.sns.gov/instruments/HFIR/HB2B/
(4) CNBC-L3 spectrometer	http://www.nrc-cnrc.gc.ca/eng/facilities/cnbc/spectrometers/l3.html
(5) SMARTS	http://lansce.lanl.gov/lujan/instruments/SMARTS/index.html [72]
(6) ISIS-ENGIN-X	http://www.isis.stfc.ac.uk/instruments/engin-x/engin-x2900.html
(7) ORNL-VULCAN	http://neutrons.ornl.gov/instruments/SNS/VULCAN/
(8) JapanSNS-TAKUMI	http://j-parc.jp/MatLife/en/instrumentation/ns_spec.html
(9) ANSTO-KOWARI	http://www.ansto.gov.au/research/bragg_institute/facilities/instruments/kowari
(10) ANSTO-WOMBAT	http://www.ansto.gov.au/research/bragg_institute/facilities/instruments/wombat

Table 3.1. Some of the website links (http://nsrc.jaea.go.jp/aonetned/index.html) of the neutron diffractometers

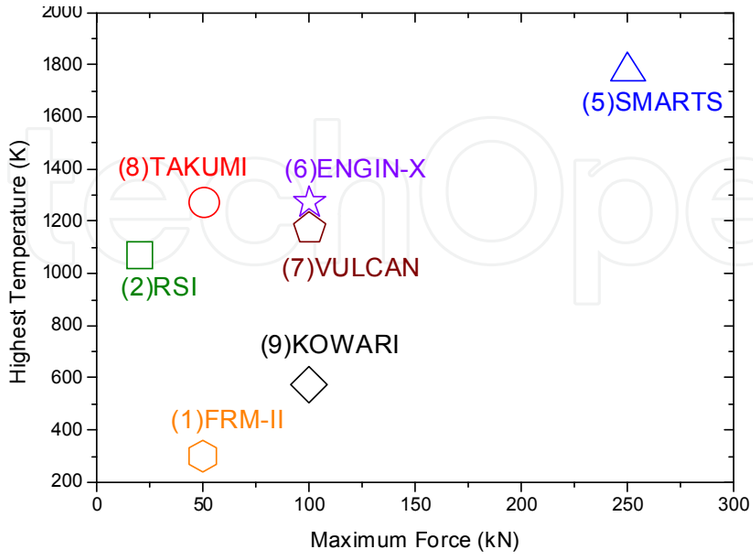

Fig. 3.1. The extreme environmental load and temperature of the neutron diffractometers summarized in Table 3.1..

3.2.5 FRM-II

Stress-Spec of the Forschungs-Neutronenquelle Heinz Maier-Leibnitz (FRM-II) is a diffractometer for residual stress and texture measurements (http://www.frm2.tum.de/en/science/diffraction/stress-spec/index.html). The capability of Stress-Spec is as good as the aforementioned diffractometers of other Reactor Neutron Source. More details can be found in Hofmann *et al.*'s introduction [71].

4. Summary

In this chapter, how to apply the neutron diffractometers to investigate the mechanical behavior of the structure materials is introduced. The applications of the neutron-diffraction experiments can reveal the lattice-strain, texture, and the microstructure evolution upon the deformation. The connections between the macroscopic-mechanical behavior and microscopic characteristics, obtained from the diffraction results, are explained. Moreover, in addition to the concepts, some of the exemplary literatures and the Neutron Engineering Diffractometers are summarized for readers' reference.

5. Acknowledgements

Particular thanks are due to Mr. Kuan-Wei Lee for his patience and careful in editing the manuscript. EWH appreciates the support from National Science Council (NSC)Program 100-2221-E-008- 2 041. JJK, EWH and Kuan-Wei Lee thank the NSC-99-3113-Y-042-001 Program.

6. References

[1] G. B. Olson, Science 277 (5330), 1237-1242 (1997).
[2] A. M.F., Acta Metallurgica 20 (7), 887-897 (1972).
[3] P. Lindner and T. Zemb, *Neutron, X-rays and light: scattering methods applied to soft condensed matter*, 1st ed. (North-Holland, 2002).
[4] G. Will, *Powder Diffraction: The Rietveld Method and the Two Stage Method to Determine and Refine Crystal Structures from Powder Diffraction Data 1st edition.* (Springer, 2006).
[5] A. C. Larson and R. B. Von Dreele, Los Alamos National Laboratory Report LAUR, 86-748 (2004).
[6] H. M. Rietveld, Acta Crystalline 22 (1967).
[7] R. W. Hertzberg, *Deformation and Fracture Mechanics of Engineering Materials*, 2nd ed. (Canada, 1976).
[8] E. W. Huang, R. I. Barabash, B. Clausen, Y.-L. Liu, J.-J. Kai, G. E. Ice, K. P. Woods and P. K. Liaw, International Journal of Plasticity 26 (8), 1124-1137 (2010).
[9] E.-W. Huang, R. I. Barabash, B. Clausen and P. K. Liaw, Metallurgical and Materials Transactions A, in press (2011). (DOI: 10.1007/s11661-011-0972-9)
[10] P. Stanley and W. K. Chan, Journal of Strain Analysis 20, 129-143 (1985).
[11] D. G. E., *Mechanical Metallurgy*, 3rd ed. (McGraw-Hill, New York, 1986).
[12] L. A. Girifalco, *Statistical Mechanics of Solids*. (Oxford University Press, 2000).
[13] A. K. Wong, S. A. Dunn and J. G. Sparrow, Nature 332 (6165), 613-615 (1988).
[14] D. Rittel, Z. G. Wang and M. Merzer, Physical Review Letters 96 (7), 075502 (2006).
[15] M. Huang, P. E. J. Rivera-Díaz-del-Castillo, O. Bouaziz and S. v. d. Zwaag, Acta Materialia 57 (12), 3431-3438 (2009).
[16] S. Quinn, J. M. Dulieu-Barton and J. M. Langlands, Strain 40 (3), 127-133 (2004).

[17] E.-W. Huang, R. Barabash, N. Jia, Y. Wang, G. E. Ice, B. Clausen, J. A. Horton Jr and P. K. Liaw, Journal Name: Metallurgical and Materials Transactions A; Journal Volume: 39A; Journal Issue: 13, 3079-3088 (2008).
[18] H. R, Journal of the Mechanics and Physics of Solids 13 (4), 213-222 (1965).
[19] J. W. Hutchinson, Acta-Scripta Metallurgica Proceedings Series 4, 12 (1989).
[20] T. Holden, C. Tomé and R. Holt, Metallurgical and Materials Transactions A 29 (12), 2967-2973 (1998).
[21] B. Clausen, T. Lorentzen, M. A. M. Bourke and M. R. Daymond, Materials Science and Engineering: A 259 (1), 17-24 (1999).
[22] B. Clausen, T. Lorentzen and T. Leffers, Acta Materialia 46 (9), 3087-3098 (1998).
[23] M. R. Daymond, C. N. Tomé and M. A. M. Bourke, Acta Materialia 48 (2), 553-564 (2000).
[24] M. R. Daymond, M. Preuss and B. Clausen, Acta Materialia 55 (9), 3089-3102 (2007).
[25] U. F. Kocks, C. N. Tome and H.-R. Wenk, *Texture and Anisotropy: Preferred Orientation in Polycrystals and Their Effects on Materials Properties*. (Cambridge University Press, 1998).
[26] Y. D. Wang, R. L. Peng and R. L. McGreevy, Philosophical Magazine Letters 81 (3), 153-163 (2001).
[27] Y. D. Wang, X.-L. Wang, A. D. Stoica, J. D. Almer, U. Lienert and D. R. Haeffner, Journal of Applied Crystallography 35 (6), 684-688 (2002).
[28] Y. D. Wang, R. L. Peng, J. Almer, M. Odén, Y. D. Liu, J. N. Deng, C. S. He, L. Chen, Q. L. Li and L. Zuo, Advanced Materials 17 (10), 1221-1226 (2005).
[29] H. Rietveld, Acta Crystallographica 22 (1), 151-152 (1967).
[30] T. Ungar, I. Groma and M. Wilkens, Journal of Applied Crystallography 22 (1), 26-34 (1989).
[31] F. J. Humphreys, Journal of Materials Science 36 (16), 3833-3854 (2001).
[32] B. R. I. and M. A. Krivoglaz, Physics of Metals 4 (1982).
[33] A. M.F, Acta Metallurgica 37 (5), 1273-1293 (1989).
[34] P. Haasen, *Physical Metallurgy*, 3rd ed. (Cambridge University Press, 1996).
[35] D. Kuhlmann-Wilsdorf, Philosophical Magazine A 79 (4), 955-1008 (1999).
[36] M. H, Acta Metallurgica 31 (9), 1367-1379 (1983).
[37] L. E. Levine, B. C. Larson, W. Yang, M. E. Kassner, J. Z. Tischler, M. A. Delos-Reyes, R. J. Fields and W. Liu, Nat Mater 5 (8), 619-622 (2006).
[38] N. Hansen, Advanced Engineering Materials 7 (9), 815-821 (2005).
[39] W. Nix, J. Gibeling and D. Hughes, Metallurgical and Materials Transactions A 16 (12), 2215-2226 (1985).
[40] Z. M, Acta Metallurgica et Materialia 41 (2), 589-599 (1993).
[41] E. Schafler, K. Simon, S. Bernstorff, P. Hanák, G. Tichy, T. Ungár and M. J. Zehetbauer, Acta Materialia 53 (2), 315-322 (2005).
[42] D. Hughes and N. Hansen, Metallurgical and Materials Transactions A 24 (9), 2022-2037 (1993).
[43] M. A. Krivoglaz, K. P. Ryaboshapka and R. I. Barabash, Physics of Meals and Metallography 30 (1970).
[44] R. I. Barabash and P. Klimanek, Journal of Applied Crystallography 32 (6), 1050-1059 (1999).
[45] R. Barabash, J. Appl. Phys. 93 (3), 1457 (2003).
[46] W. T. Read and W. Shockley, Physical Review 78 (3), 275 (1950).
[47] A. Ardell, Metallurgical and Materials Transactions A 16 (12), 2131-2165 (1985).
[48] A. Wilm, Metallurgie 8, 225-227 (1911).
[49] E. Huang, P. K. Liaw, L. Porcar, Y. Liu, J. Kai and W. Chen, Appl. Phys. Lett. 93 (16), 161904 (2008).
[50] S. H. Chen, Annual Review of Physical Chemistry 37 (1), 351-399 (1986).

[51] J. S. Pedersen, Physical Review B 47 (2), 657 (1993).
[52] R. Giordano, A. Grasso, J. Teixeira, F. Wanderlingh and U. Wanderlingh, Physical Review A 43 (12), 6894 (1991).
[53] S. Y. Lee, H. Choo, P. K. Liaw, E. C. Oliver and A. M. Paradowska, Scripta Materialia 60 (10), 866-869 (2009).
[54] S. Y. Lee, M. A. Gharghouri and J. H. Root, presented at the TMS, San Diego, California, 2011 (unpublished).
[55] E. C. Oliver, M. R. Daymond and P. J. Withers, Acta Materialia 52 (7), 1937-1951 (2004).
[56] M. A. M. Bourke, D. C. Dunand and E. Ustundag, Applied Physics A: Materials Science & Processing 74 (0), s1707-s1709 (2002).
[57] S. R. Agnew, J. A. Horton, T. M. Lillo and D. W. Brown, Scripta Materialia 50 (3), 377-381 (2004).
[58] W. Woo, Z. Feng, X. L. Wang, D. W. Brown, B. Clausen, K. An, H. Choo, C. R. Hubbard and S. A. David, Science and Technology of Welding & Joining 12 (4), 298-303 (2007).
[59] P. J. Withers and H. K. D. H. Bhadeshia, Materials Science and Technology 17 (4), 366-375 (2001).
[60] M. T. Hutchings, P. J. Withers, T. M. Holden and T. Lorentzen, *Introduction to the characterization of residual stress by neutron diffraction*, 1st ed. (Taylor and Francis, London, 2005).
[61] Y. Tomota, H. Tokuda, Y. Adachi, M. Wakita, N. Minakawa, A. Moriai and Y. Morii, Acta Materialia 52 (20), 5737-5745 (2004).
[62] W. Woo, Z. Feng, X. Wang and S. A. David, Science and Technology of Welding & Joining 16 (1), 23-32 (2011).
[63] S. Y. Lee, P. K. Liaw, H. Choo and R. B. Rogge, Acta Materialia 59 (10), 4253 (2011).
[64] S. Y. Lee, H. Choo, P. K. Liaw, K. An and C. R. Hubbard, Acta Materialia 59 (10), 4254 (2011).
[65] W. Woo, H. Choo, M. B. Prime, Z. Feng and B. Clausen, Acta Materialia 56 (8), 1701-1711 (2008).
[66] W. Woo, H. Choo, D. W. Brown, P. K. Liaw and Z. Feng, Scripta Materialia 54 (11), 1859-1864 (2006).
[67] W. Woo, V. Em, B.-S. Seong, E. Shin, P. Mikula, J. Joo and M.-H. Kang, Journal of Applied Crystallography 44 (4), 747-754 (2011).
[68] W. Woo, V. Em, C. R. Hubbard, H.-J. Lee and K. S. Park, Materials Science and Engineering: A 528 (27), 8021-8027 (2011).
[69] W. Woo, Z. Feng, X. L. Wang and C. R. Hubbard, Scripta Materialia 61 (6), 624-627 (2009).
[70] E-W. Huang, S. Y. Lee, W. Woo, and K-W. Lee, Metallurgical and Materials Transactions A (2011). (DOI: 10.1007/s11661-011-0904-8).
[71] M. Hofmann, R. Schneider, G. A. Seidl, J. Rebelo-Kornmeier, R. C. Wimpory, U. Garbe and H. G. Brokmeier, Physica B: Condensed Matter 385-386, Part 2 (0), 1035-1037 (2006).
[72] M. A. M. Bourke, D. C. Dunand and E. Ustundag, Applied Physics A: Materials Science & Processing 74 (0), s1707-s1709 (2002).

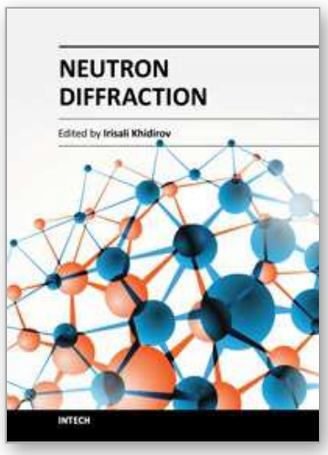

Neutron Diffraction

Edited by Prof. Irisali Khidirov

ISBN 978-953-51-0307-3
Hard cover, 286 pages
Publisher InTech
Published online 14, March, 2012
Published in print edition March, 2012

Now neutron diffraction is widely applied for the research of crystal, magnetic structure and internal stress of crystalline materials of various classes, including nanocrystalls. In the present book, we make practically short excursion to modern state of neutron diffraction researches of crystal materials of various classes. The book contains a helpful information on a modern state of neutron diffraction researches of crystals for the broad specialists interested in studying crystals and purposeful regulation of their service characteristics, since the crystal structure, basically, defines their physical and mechanical properties. Some chapters of the book have methodical character that can be useful to scientists, interested in possibilities of neutron diffraction. We hope, that results of last years presented in the book, can be a push to new ideas in studying of crystalline, magnetic structure and a macrostructure of usual crystal materials and nanocrystals. In turn, it can promote working out of new materials with new improved service characteristics and to origin of innovative ideas.

How to reference

In order to correctly reference this scholarly work, feel free to copy and paste the following:

E-Wen Huang, Wanchuck Woo and Ji-Jung Kai (2012). Introduction of Neutron Diffractometers for Mechanical Behavior Studies of Structural Materials, Neutron Diffraction, Prof. Irisali Khidirov (Ed.), ISBN: 978-953-51-0307-3, InTech, Available from: http://www.intechopen.com/books/neutron-diffraction/introduction-of-neutron-diffractometers-for-mechanical-behavior-studies-of-structural-materials

INTECH
open science | open minds

InTech Europe
University Campus STeP Ri
Slavka Krautzeka 83/A
51000 Rijeka, Croatia
Phone: +385 (51) 770 447
Fax: +385 (51) 686 166
www.intechopen.com

InTech China
Unit 405, Office Block, Hotel Equatorial Shanghai
No.65, Yan An Road (West), Shanghai, 200040, China
中国上海市延安西路65号上海国际贵都大饭店办公楼405单元
Phone: +86-21-62489820
Fax: +86-21-62489821

IntechOpen